

Effect of Aromatic Diamine Extenders on the Morphology and Property of RIM Polyurethane-Urea

YUN GAO,* YU-YING XIU, ZHAO-QI PAN, DE-NING WANG, CHUN-PU HU, and SHENG-KANG YING

Institute of Polymer Science and Engineering, East China University of Science and Technology, Shanghai 200237, People's Republic of China

SYNOPSIS

An aromatic diamine, CMOMDA, was synthesized and used as a chain extender for reaction injection molding (RIM) polyurethane-urea. The morphology and properties of CMOMDA-, DETDA-, and MDA-extended poly(ether-urethane-urea)s (PEUUs) were measured by IR, DSC, DMS, SEM, and tensile testing apparatus. Well-matched values of C_h and $X_{ut,b}/C_h$ were necessary for aromatic diamine-extended PEUU. DSC and SEM showed that the aggregation state of hard segments might undergo some changes with increasing hard-segment content. © 1994 John Wiley & Sons, Inc.

INTRODUCTION

Reaction injection molding (RIM) is an important technique of polymer reactive processing. There is much literature about the structure and properties of RIM polyurethane (PU), whereas fundamental investigations on RIM polyurethane-urea (PUU), in comparison with RIM PU, are less reported. Segmented poly(ether-urethane-urea) (PEUU) copolymers are composed of alternating soft- and hard-segment blocks. The soft-segment block is polyether, and the hard-segment block is constituted from low molecular weight diamine as a chain extender, for which the most useful is the aromatic diethyltoluenediamine (DETDA). Phase separation of segmented PEUU due to thermodynamic incompatibility between the soft and hard segments is well known. The hard segment, composed of the reaction products of diisocyanate and diamine, can noncovalently self-associate to form domains that act as physical cross-links for reinforcing the polymers. Some researchers¹⁻⁸ have examined the effects of a chain extender on the structure, morphology, and properties of PUU by solution, prepolymer, or model polymer synthesis. This study pays attention to the one-shot, bulk-polymerized PEUU containing trifunctional poly(ether polyol) and aromatic diamine.

EXPERIMENTAL

Synthesis

Segmented PEUUs were synthesized by impingement mixing of urethonimine-modified 4,4'-methylenebis(phenylene isocyanate) (L-MDI) as the A component stream and premixed poly(ether polyol), diamine chain extender, and catalysts as the B component stream. The temperature of stoichiometric components was 40°C. A laboratory-scale RIM machine, designed by our research group, was used for mold (200 × 100 × 3) filling. The temperature of the mold was maintained at 70°C. The solidified sample was taken off the mold 30 s after mold filling and then was annealed at 120°C for 1 h.

L-MDI (average functionality, 2.13; —NCO content, 28.72% by weight) was degassed under vacuum conditions. The poly(oxypropylene-oxyethylene)triol (average functionality 3, [OH] equivalent 31.99 mg KOH/g) was dewatered under vacuum. The catalysts, dibutyltin dilaurate and triethylenediamine, were used as received.

Diethyltoluenediamine (DETDA), the most useful chain extender in the commercial scale, was supplied by Ethyl Chemical Corp. and 4,4'-diaminodiphenylmethane (MDA) by Shanghai Reagent Factory No. 2. 3-Chloro,3'-methoxy,4,4'-diaminodiphenylmethane (CMOMDA) was synthesized according to the literature.⁹

* To whom correspondence should be addressed.

Methods

An FTIR instrument, a Nicolet 20SX, recorded the ATR spectra of PEUU samples for studying the hydrogen-bonding behavior. DSC thermograms over the temperature range -80 to 240°C were recorded using a DuPont 1090. The experiments were carried out at a heating rate of $20^{\circ}\text{C}/\text{min}$ under N_2 purge. Sample weights were 10–20 mg. SEM on an S-250MKII apparatus was used for fracture surface appearance examination after the fracture surface had been coated by a gold vapor. For observation of phase separation phenomena, the PEUU samples were selectively etched by DMF–chloroform solvent vapor at room temperature before they were coated by a gold vapor. Dynamic mechanical data were collected at 11 Hz at a $2^{\circ}\text{C}/\text{min}$ heating rate in the temperature range -100 – 200°C with a DDVIII viscoelasticimeter. Stress–strain experiments were done with an Autograph AG-2000A tensile testing apparatus with a crosshead speed of 50 mm/min.

RESULTS AND DISCUSSION

Effects of Different Chain Extenders

Relative Activity

Synthesis of PEUU is an exothermic process. Figure 1 shows the adiabatic temperature increase curves of PEUUs with 43% (by weight) hardblock content.

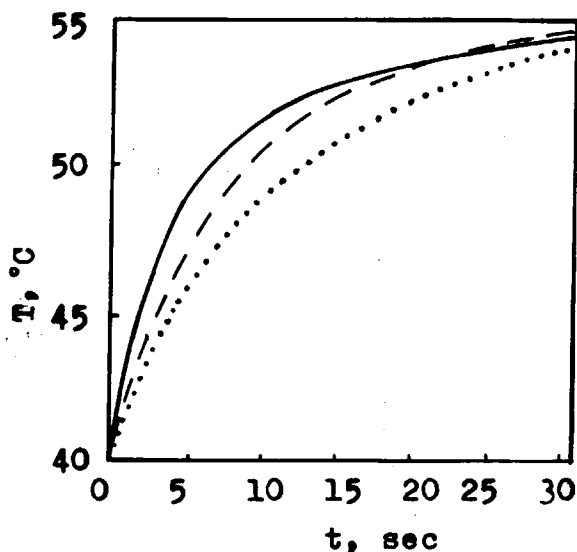


Figure 1 The adiabatic temperature increase curves of PEUUs with different chain extenders: (—) MDA; (----) DETDA; (· · · · ·) CMOMDA.

Table I The Relative Activity of Each Chain Extender

	MDA	DETDA	CMOMDA
K	0.20	0.14	0.08
Relative activity	1.43	1.00	0.57

According to the literature,¹⁰ the relative activity of the chain extender could be calculated as follows:

$$(dT/dt)_{t \rightarrow 0} = K \Delta T_{ad} \quad (1)$$

$$K = (dT/dt)_{t \rightarrow 0} / \Delta T_{ad} \quad (2)$$

where ΔT_{ad} is the maximum adiabatic temperature increase value ($^{\circ}\text{C}$) and K is a factor depending on the reaction activity of the chain extender. The K values and relative activity of each chain extender in this study are listed in Table I.

From Figure 1 and Table I, it was observed that MDA and CMOMDA were more and less reactive than DETDA, respectively, which might be attributed to the steric hindrance and the electric charge distribution on the $-\text{NH}_2$ group.

Hydrogen Bonding

The IR spectra of PEUU samples are shown in Figure 2. The NH absorptions (peak at 3310 cm^{-1}) were nearly completely hydrogen-bonded for all the samples. In the carbonyl region, the peak at 1646 cm^{-1} is the hydrogen-bonded urea carbonyl ($\text{CO}_{\text{ua,b}}$), the peak located at 1730 cm^{-1} is due to free urethane carbonyl ($\text{CO}_{\text{ut,f}}$), and the peak at 1715 cm^{-1} is the hydrogen-bonded urethane carbonyl ($\text{CO}_{\text{ut,b}}$). A free urea carbonyl peak at 1705 cm^{-1} was not detected. Define

$$X_{\text{ut,b}} = A_{\text{CO}_{\text{ut,b}}} / (A_{\text{CO}_{\text{ut,b}}} + A_{\text{CO}_{\text{ut,f}}}) \quad (3)$$

$$C_h = A_{\text{CO}_{\text{ua,b}}} / A_{\text{ref}} \quad (4)$$

where $X_{\text{ut,b}}$ is the ratio of the absorbance peak area of the hydrogen-bonded urethane carbonyls to that

Table II Hydrogen-bonding Behavior of PEUUs

Chain Extender	$X_{\text{ut,b}}$	C_h	$X_{\text{ut,b}}/C_h$
MDA	0.58	1.49	0.38
DETDA	0.48	1.06	0.45
CMOMDA	0.52	0.70	0.74

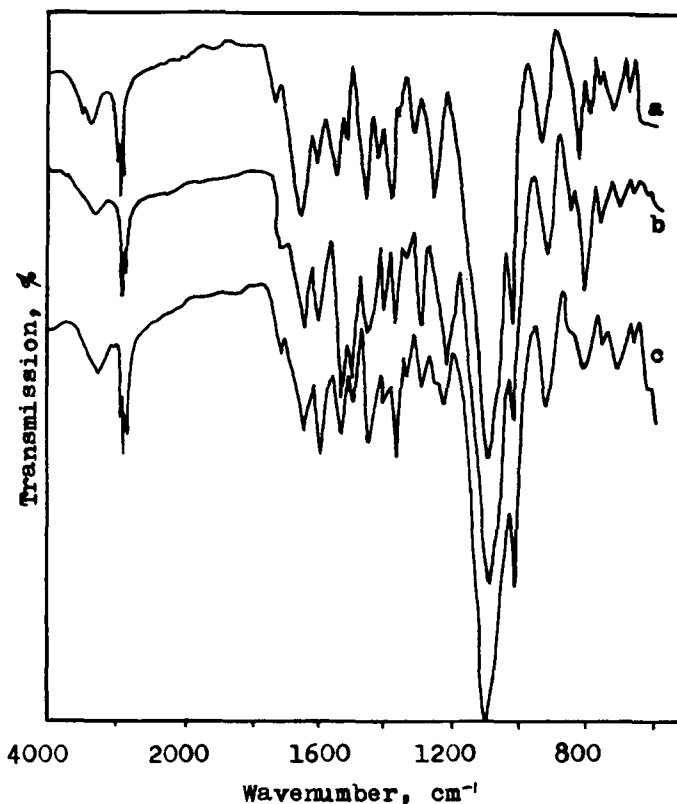


Figure 2 Infrared spectra of PEUU samples with different chain extenders: (a) MDA; (b) DETDA; (c) CMOMDA.

of all urethane carbonyls that link up the polyether soft segments. C_h is the ratio of the absorbance peak area of hydrogen-bonded urea carbonyls to that of the C=C stretching absorption of the benzene ring at 1600 cm^{-1} as the reference peak (A_{ref}). C_h could be used as an index of the degree of the inter-hard-

segment cohesive force. The ratio of $X_{ut,b}/C_h$ could be used to stand for an index of the interfacial interaction between soft- and hard-segment domains.^{7,11}

From Table II, the PEUU made from MDA has a stronger cohesive force of hard segments and shows weaker interfacial interaction between soft- and hard-segment domains than that from DETDA, whereas PEUU from CMOMDA is the reverse.

Phase Separation

Figure 3 shows the DSC thermograms of the PEUU samples. The transition temperatures are listed in Table III.

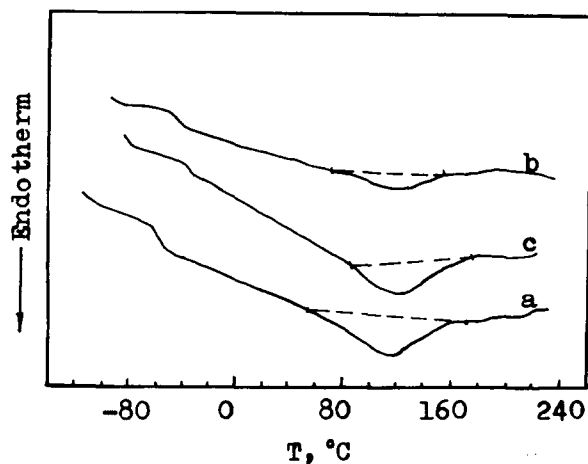


Figure 3 DSC curves of PEUU samples with different chain extenders: (a) MDA; (b) DETDA; (c) CMOMDA.

Table III DSC Data of PEUU Samples

Sample	T_g 's (°C)	ODT (°C)	ΔH (J/g)
MDA	-57.1	117.0	26.4
DETDA	-52.1	119.5	11.9
CMOMDA	-40.2	120.7	18.6

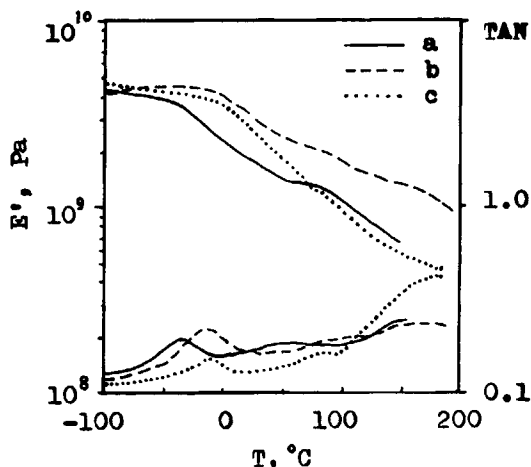


Figure 4 The dynamic mechanical spectroscopy of PEUUs with different chain extenders: (a) MDA; (b) DETDA; (c) CMOMDA.

The vitrification point of soft segments, T_g 's, could serve as a reasonable criterion for the degree of phase separation, when all samples contained the same amount of hard segments (here 43% by weight).¹² The T_g 's of the PEUU sample from MDA was lower than that from DETDA and the T_g 's of the sample from CMOMDA is higher than from DETDA. These suggested that the phase separation between hard and soft segments was more developed in the MDA-extended sample and less developed in the CMOMDA-extended sample than in the DETDA-extended sample. The glass transition temperatures of all the samples were higher than the T_g 's of the pure soft-segment oligomer, indicating that there is some mixing of hard segments into the soft-segment microphase. Moreover, all the DSC curves show a broad endothermic transition at 120°C (order-disorder transition [ODT]), and this might be the ODT discussed by Anthony et al.¹³ The broad transition resulted from the wide distribution of hard-segment sequence lengths.

The dynamic mechanical data are presented in Figure 4 and Table IV. The T_g 's determined by the dynamic mechanical modulus is generally higher than that by DSC. Ignoring the different test meth-

Table IV Dynamic Mechanical Data

Sample	T_g 's (°C)	$E'(-30^\circ\text{C})/E'(+65^\circ\text{C})$
MDA	-51.0	2.9
DETDA	-32.5	2.0
CMOMDA	-27.2	3.5

Table V Tensile Strength Data

Sample	Tensile Strength (Mpa)	Elongation at Break (%)	Density (g/cm ³)
MDA	Brittle and crack in sample		0.96
DETDA	14.3	194	0.98
CMOMDA	10.0	103	0.94

ods, the sequence of T_g values were in agreement with the data resulting from DSC, i.e., CMOMDA > DETDA > MDA.

From the above-described phenomena, the conclusion could be drawn that hydrogen bonding of hard segments and phase separation would be more developed for the PEUU sample containing a chain extender of a higher reaction activity.

Tensile Stress-Strain

Table V shows the tensile strength data. The MDA-extended PEUU sample was too brittle to test the tensile stress-strain, which might be attributed to the extraordinarily fast reaction of MDA with L-MDI, so that the value $X_{ut,b}/C_h$ was very low. Figure 5(a) is the SEM image of its fracture surface. Clearly, there were cavities on the fracture surface from which hard-segment-rich particles had been pulled out by stretching the sample. This offered evidence for a weak interaction between hard-segment- and soft-segment-rich domains of MDA-extended PEUU.

Figure 5(b) and (c) shows the fracture surfaces of DETDA- and CMOMDA-extended PEUU, respectively. Traces showing laceration by a strong tensile force could be observed on the fracture surfaces. The cavities on the fracture surfaces were not as smooth and regular as Figure 5(a) showed, but coarse and odd-shaped, which resulted from tensile failure. This means that the interaction between

Table VI DSC Data of CMOMDA-extended PEUUs with Different Hard-segment Contents

Sample	Hard-segment Content (Wt %)	T_g 's (°C)	ODT (°C)	ΔH (J/g)
CMOMDA-10	10	-51.4	—	—
CMOMDA-20	20	-47.3	123.7	9.8
CMOMDA-30	30	-42.8	132.7	17.5
CMOMDA-45	45	-38.3	127.9	19.9

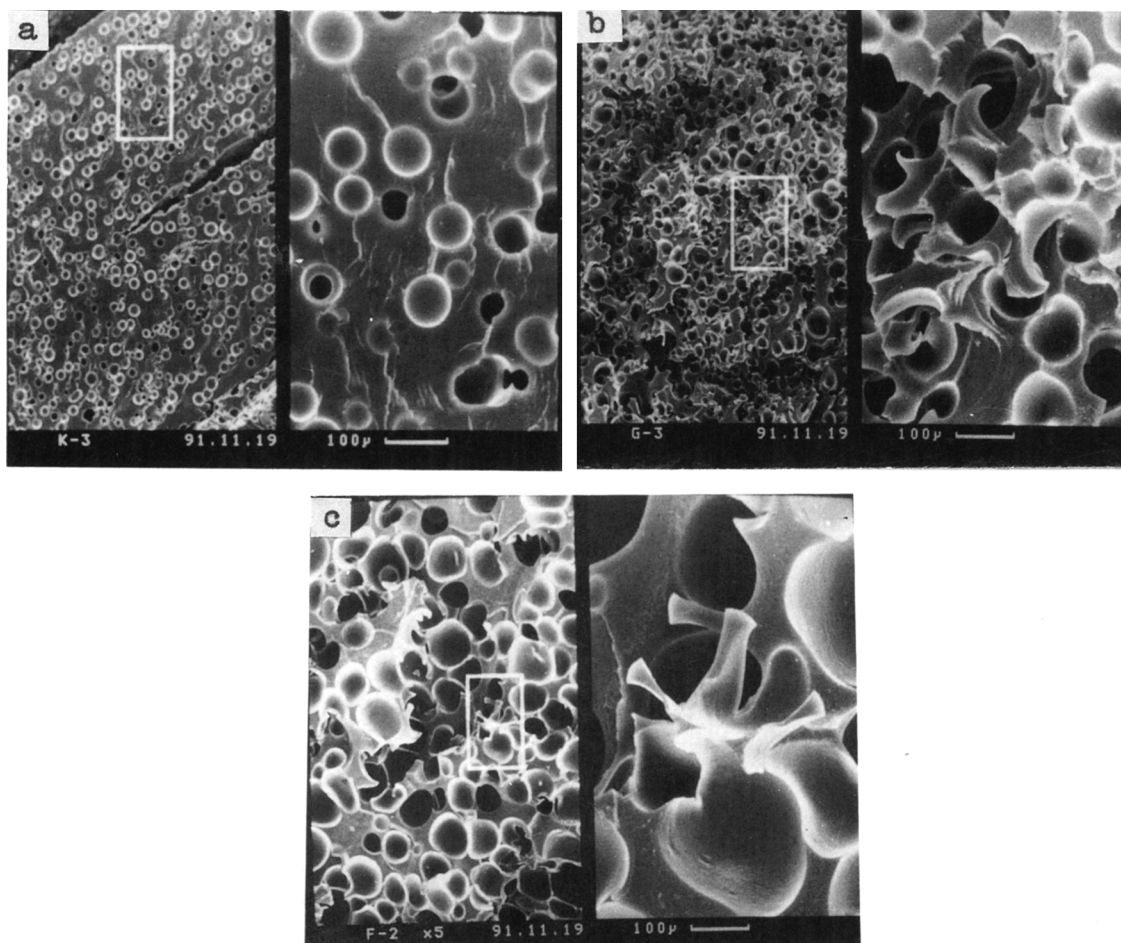


Figure 5 SEM micrographs of PEUU samples with different chain extenders: (a) MDA; (b) DETDA; (c) CMOMDA.

hard-segment- and soft-segment-rich domains were somewhat stronger in DETDA- and CMOMDA-extended PEUU than in MDA-extended PEUU.

By comparing the tensile stress-strain and $E'(-30^{\circ}\text{C})/E'(+65^{\circ}\text{C})$ data in Tables IV and V with the hydrogen-bonding behavior in Table II, one could conclude that well-matched values of C_h and $X_{ut,b}/C_h$ were necessary for diamine-extended PEUU, which means that the C_h value should be in

a coordinated and compatible fashion with the value of $X_{ut,b}/C_h$.

Effects of Hard-segment Contents (Samples Prepared by Stirrer Mixing)

Figure 6 shows the DSC thermograms of CMOMDA-extended PEUU samples with different

Table VII Mechanical Properties of CMOMDA-extended PEUUs

Sample	Hard-segment Content (Wt %)	Modulus (Mpa)	Tensile Strength (Mpa)	Elongation at Break (%)
CMOMDA-10	10	0.22	0.63	280.8
CMOMDA-20	20	0.52	1.83	280.2
CMOMDA-30	30	3.88	5.97	210.4
CMOMDA-45	45	70.73	20.51	80.4

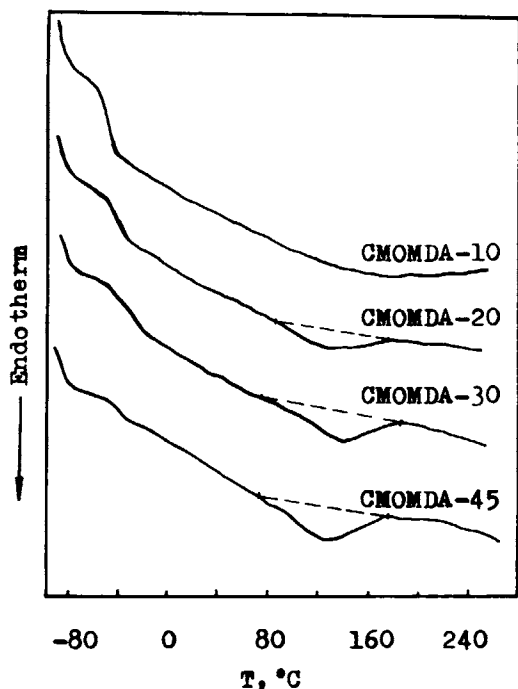


Figure 6 DSC curves of PEUU with different hard-segment contents.

hard-segment contents (by weight). The thermal characteristics are listed in Table VI.

The T_g 's and ΔH of the *ODT* increased with increasing hard-segment content, but no *ODT* was detected for sample with only 10% hard-segment content. This means that more hard segments became mixed into the soft-segment microphase and that the state of aggregation of hard segments could also undergo some changes with an increasing amount of CMOMDA. Figure 7 shows the SEM microphotos of PEUUs with different amounts of the CMOMDA chain extender. The dark regions are soft-segment-rich domains, whereas the bright regions are hard-segment-rich domains.

In Figure 7(a), the hard-segment-rich domains were distributed clearly as striations in the soft-segment matrix and the SEM image appeared as a lamellar structure. In Figure 7(b), the hard-segment-rich domains became a cross network and were packed more closely than in Figure 7(a). In Figure 7(c), as the hard-segment content increased to 45%, the hard-segment-rich domains took further steps to aggregate compactly, tending to form a spherular superstructure. By changing the aggregation state

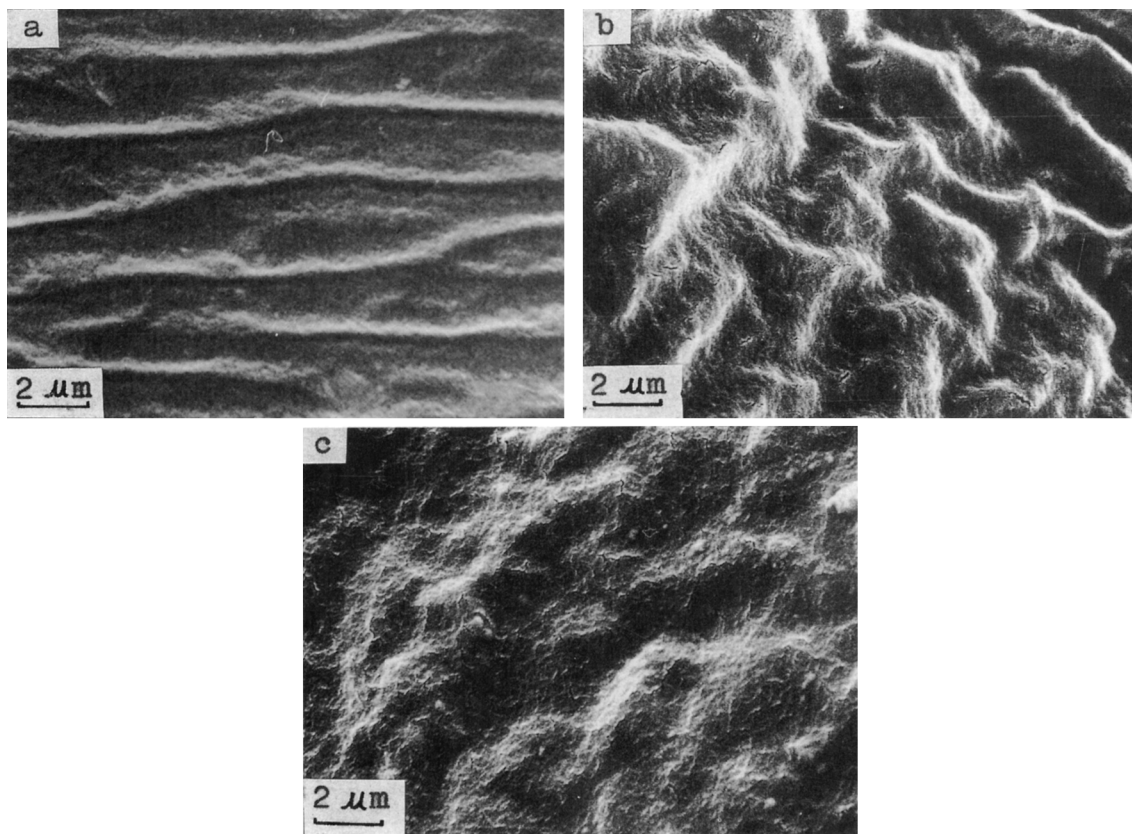


Figure 7 SEM microphotographs of CMOMDA-extended PEUU with different hard-segment content: (a) 20%; (b) 30%; (c) 45%.

of hard segments, the CMOMDA-extended PEUUs showed different mechanical properties (Table VII). The general trend of mechanical property variations was in agreement with DETDA-extended PEUU.¹⁴

The study was supported by the National Natural Science Foundation of China.

REFERENCES

1. C. Hepburn and J. W. Reynolds, *Elastomer: Criteria for Engineering Design*, Applied Science, London, 1982, p. 323.
2. C. B. Hu, R. S. Wards, and N. S. Schneiders, *J. Appl. Polym. Sci.*, **27**, 2167 (1982).
3. B. W. Carl and L. C. Stuart, *Macromolecules*, **16**, 775 (1983).
4. E. M. Charles, G. E. Peter, and D. R. Buddy, *Appl. Spectrosc.*, **24**(4), 576 (1990).
5. J. Born and H. Hespe, *Colloid Polym. Sci.*, **263**, 335 (1985).
6. I. Hideaki and R. Itsuro, *J. Macromol. Sci.-Phys.*, **B22**(5,6), 713 (1983-1984).
7. S. Mitsuhiro, K. Toshihito, K. Tetsuo, N. Shunji, and M. Takehisa, *Polym. J.*, **18**(10), 719 (1986).
8. Y. Tomoyuki, S. Mitsuhiro, and N. Shynji, *Polym. J.*, **21**(11), 895 (1989).
9. Y. Gao, D. I. Wang, and S. K. Ying, *Chem. J. Chin. Univ.*, **14**(8), 1176 (1993).
10. D. Nissen and R. A. Markovs, *J. Elastomers Plast.*, **15**(2), 96 (1983).
11. Y. K. Wang and X. LI, in *Symposium on Polymers*, Wuhan, China, Oct. 13-17, 1987, Vol. 2, p. 765.
12. P. E. Gibson and S. L. Cooper, *J. Polym. Sci. Polym. Phys. Ed.*, **21**, 65 (1983).
13. J. R. Anthony, W. M. Christopher, and B. Wim, *Macromolecules*, **25**, 6277 (1992).
14. A. J. Birch, J. L. Stanford, and A. J. Ryan, *Polym. Bull.*, **22**, 629 (1989).

Received September 20, 1993

Accepted December 15, 1993